Title:

"Activity-dependent control of inhibitory interneuron number in the mammalian cortex"

Myrto Denaxa[1],*, Guilherme Neves[2],*, Adam Rabinowitz[3], Sarah Kemlo[2], Petros Liodis[4], Juan Burrone[2],& and Vassilis Pachnis[1],&

[1]Nervous System Development and Homeostasis Laboratory, The Francis Crick Institute, 1 Midland Road, London NW1 1AT, United Kingdom

[2]Centre for Developmental Neurobiology, King's College London, New Hunt's House, 4th Floor, Guy's Hospital Campus, London, SE1 1UL, United Kingdom

[3]Bioinformatics and Biostatistics Laboratory, The Francis Crick Institute, 1 Midland Road, London NW1 1AT, United Kingdom

[4]Molecular Neurobiology, NIMR, The Ridgeway, Mill Hill, London, NW7 1AA, United Kingdom

*These authors contributed equally to the work.

&Equal contribution and authors for correspondence: Vassilis.Pachnis@crick.ac.uk and juan.burrone@kcl.ac.uk

Summary

Cortical networks are composed of excitatory projection neurons and inhibitory interneurons. Although fewer in number relative to projection neurons, interneurons have essential roles in brain activity and behavior since they adjust cortical excitation and control network dynamics. Therefore, the number of cortical interneurons (CIs) must be tightly controlled during development to meet the functional requirements of emerging neuronal circuits. CIs are generated in excess from basal forebrain progenitors and it has been proposed recently that their final number is adjusted via intrinsically determined apoptosis occurring during an early postnatal window. Here we provide evidence that the extent of CI apoptosis during this critical period is plastic, cell type specific and can be reduced in a cell autonomous manner by acute increases in neuronal activity. We further show that hyperactive networks promote the survival of transplanted CIs. We propose that the level of activity in emerging neural networks controls in a homeostatic manner the number of CIs.

Introduction

The balance between excitation and inhibition (E-I balance) is essential for the generation of optimal neural circuit activity patterns and brain function. Cortical interneurons (CIs) represent the main source of inhibition for excitatory projection neurons (PNs) in the pallium and changes in the number or activity of CIs have been associated with neurodevelopmental and neuropsychiatric disorders, such as epilepsy, Rett syndrome, schizophrenia and autism spectrum (ASD) disorders (Marin, 2012; Rubenstein and Merzenich, 2003). In contrast to cortical PNs, which are generated in the germinal zones of the dorsal telencephalon, CIs originate from progenitors in the

medial and caudal ganglionic eminences (MGE and CGE, respectively), and the preoptic area (POA) of the subpallium and following stereotypic migration routes integrate into cortical circuits (Wonders and Anderson, 2006; Welagen and Anderson 2011). The disparate sites of origin of cortical PNs and CIs raise questions regarding the mechanisms that control the relative size of the two neuronal populations and the E-I balance of mature cortical circuits. A recent report has demonstrated that CIs are generated in excess from basal forebrain progenitors and that apoptosis occurring over a critical postnatal (P) stage adjusts the final number of inhibitory neurons (Southwell et al., 2012). Nevertheless, it remains unclear whether the programme of apoptosis, unfolding during a developmental period characterised by marked neural plasticity, is controlled by mechanisms intrinsic to the population of CIs, or can be modulated by changes in the activity of the emerging cortical circuits and the physiological status of the postnatal brain.

A potential experimental strategy to address these questions in mammals entails assessment of CI populations in mouse mutant strains characterised by reproducible changes in the cellular microenvironment and activity of the cortex. Systematic gene expression analysis, genetic cell lineage tracing and phenotypic characterisation of mutant mice have demonstrated that CI subtypes are determined by distinct and region-specific transcriptional programmes operating within progenitor domains of the subpallium (Fishell and Rudy, 2011). *Lhx6* encodes a LIM homeodomain transcription factor, which is specifically expressed by MGE derived CI precursors and their derivative interneurons identified by the expression of somatostatin and parvalbumin (Sst^+ and Pv^+). Consistent with its expression, *Lhx6* mutations are characterised by mild and transient delay in early tangential migration of CI precursors and severe reduction in the number of Sst^+ and Pv^+ CIs (Liodis et al.

2007; Zhao et al., 2008). These cellular phenotypes are associated with reduced inhibitory synaptic input on PNs, brain hyperactivity and epilepsy-like phenotypes in postnatal animals (Neves at al., 2013). By combining phenotypic analysis and genetic lineage tracing of MGE- and CGE-derived CIs in mutant mice with lineage tracing and chemogenetic activation of transplanted CI precursors, we provide evidence that the programmes of apoptosis of inhibitory cortical neurons during a critical postnatal period are not intrinsically hard-wired but can be modulated by network activity and the excitability of individual neurons.

Results

Loss of MGE CIs results in a compensatory increase in the number of CGE CIs.

To determine whether changes in the cellular microenvironment or physiological state of the postnatal forebrain modulate the extent of CI apoptosis in postnatal brain, we first employed genetic lineage tracing to assess the effects of *Lhx6* ablation on distinct subpopulations of CIs. Combination of a previously reported null allele of *Lhx6* (*Lhx6*$^{-}$) (Liodis et al., 2007) and a novel conditional (floxed) mutation of the locus (*Lhx6*^{fl}; Figure S1) with the MGE-specific *Nkx2.1Cre* driver (Kessaris et al., 2006) and the Cre-dependent tdTomato reporter (tdT; Ai14) (Madisen et al., 2010) allowed us to ablate *Lhx6* specifically from MGE CIs and simultaneously fate-map the mutant cell lineages. The number of MGE-derived (tdT^{+}) CIs in the cortex of P18 *Nkx2.1Cre;Ai14;Lhx6*$^{fl/-}$ mice was dramatically reduced in comparison to control littermates (*Nkx2.1Cre;Ai14;Lhx6*$^{fl/+}$; Figure 1A, 1B, 1G and S2A). These findings suggest that *Lhx6* activity is required for the survival and thus the development of a normal complement of MGE CIs. Using biosynthetic enzymes of the common inhibitory neurotransmitter γ-amino butyric acid (GABA), we and others have

reported that the total number of CIs remained unchanged in two independently generated *Lhx6* null mutants (Liodis et al., 2007; Zhao et al., 2008). In further support of these findings, we demonstrate here that the number of cells identified by the panCI *VgatCre;Ai14* transgenic driver and reporter combination (Vong et al., 2011) was similar in *Lhx6*$^{fl/-}$ and *Lhx6*$^{fl/+}$ P18 cortices (Figure 1C, 1D, 1H). To resolve the apparent contradiction between these sets of data, we next fate-mapped CGE-derived CIs in *Lhx6* null mutants using a CGE-specific *Htr3αCre* transgene in combination with the tdT reporter. Surprisingly, we observed a significantly higher number of CGE-derived tdT^{+} cells in the cortex of *Lhx6* null mice (*Htr3aCre;Ai14;Lhx6*$^{-/-}$) relative to controls (*Htr3aCre;Ai14;Lhx6*$^{+/-}$) (Figure 1E, 1F, 1I and Figure S2D). As described previously (Vogt et al., 2014), 5.9 ± 0.4 % of MGE CIs in Lhx6-deficient brains expressed markers typical of CGE CI fate (Figure S1I, S1J), but this presumed change in cell fate could not explain the large increase in CGE CIs observed in mutant animals. Together these data suggest that the size of the CGE-derived interneuron population in the postnatal mammalian cortex is dynamic and increases in an apparent compensatory response to deficits in the counterpart population of MGE CIs.

CGE CIs include two major non-overlapping sub-populations which are marked by Vasoactive Intestinal Peptide [VIP; involved in disinhibitory circuit motifs (Kepecs and Fishell, 2014)] and Reelin [neurogliaform cells associated with volume transmission (Fishell and Rudy, 2011; Lee et al., 2010)]. Immunostaining of brain sections from *Htr3aCre;Ai14;Lhx6*$^{-/-}$ mice using these subtype-specific markers showed that the compensatory response of CGE CIs was due specifically to an increase in the number of Reelin^{+} CIs (Figure 1J, 1K and Figure S2E, S2F). Interestingly, the number of non MGE- or CGE-derived Pv^{+} CIs, which are likely to originate from the preoptic area (POA) (Gelman et al., 2011) (Figure S3), also

increased in *Lhx6* mutant cortices, whereas Sst^{+} CIs generated outside the MGE remained unchanged (Figure 1L, 1M and Figure S2B, S2C). These findings argue that the compensatory survival of CIs is not restricted to CGE-derived lineages and is subtype specific.

Reciprocal changes in apoptosis of CGE and MGE CIs in Lhx6 mutants

Changes in CI number could arise from altered cell proliferation and migration during embryogenesis, or changes in neuronal cell death during the critical postnatal window of apoptosis (Southwell et al., 2012; Yamaguchi and Miura, 2015). We detected no changes in MGE or CGE progenitor proliferation or in the tangential migration of CGE CI precursors in the forebrain of E14-16 *Lhx6*$^{-/-}$ embryos (Figure S4). Consistent with this, the number of MGE- and CGE-derived CIs at P2 (a stage that follows the completion of tangential migration of CIs to the pallium but precedes the onset of apoptosis (Miyoshi and Fishell, 2011; Southwell et al., 2012) was similar between control and mutant mice (Figure 2A-D and 2I). In contrast, the corresponding numbers at P7 were significantly higher (for CGE CIs) or lower (for MGE CIs) in *Lhx6*$^{-/-}$ animals relative to controls (Figure 2E-H and 2I), suggesting that the reciprocal changes of these populations observed at P18 (Figure 1G, 1I and Figure 2I) result from altered rates of apoptosis in mutant mice. To confirm this, we compared rates of apoptosis of CIs in the cortex of *Lhx6* null mutants and controls at P7, a stage characterised by the highest levels of CI cell death. We observed a significant reduction in the number of Lhx6-independent CGE CIs undergoing programmed cell death (TUNEL^{+}) in *Htr3aCre;Ai14;Lhx6*$^{-/-}$ in comparison to controls (*Htr3aCre;Ai14;Lhx6*$^{+/-}$) and a clear trend for increase of the TUNEL^{+} fraction of Lhx6-dependent MGE CIs between *Nkx2.1Cre;Ai14;Lhx6*$^{fl/-}$ and their control

littermates (*Nkx2.1Cre;Ai14;Lhx6*$^{fl/+}$; Figure 2J-L). Based on these experiments, we suggest that modulation of apoptosis drives the dynamic responses of CI subpopulations to the changes in the postnatal forebrain associated with *Lhx6* mutations.

Hyperactivity of Lhx6 mutants promotes grafted CI precursor survival.

We have previously demonstrated a decreased inhibitory input in *Lhx6* null mutant (Neves et al, 2013). To characterise the molecular changes associated with forebrain hyperexcitability in *Lhx6* mutants we carried out transcriptome analysis of Lhx6-deficient brains at P15 using mRNA sequencing. These experiments showed up-regulation of genes (*Bdnf*, *Npas4*, *Fosb*, *Npy*) and pathways (MAPK signalling, calcium signalling) typically associated with increased network activity (Figure S5). The list of up-regulated genes in the absence of Lhx6 function was highly enriched in genes that are up-regulated in pyramidal neurons following chronic inhibition of ionotropic GABA receptors, as shown by hypergeometric test analysis (FDR<10^{-59}; Yu et al., 2015). Interestingly, the up-regulation of the neuronal activity markers such as c-fos and Arc, was already evident at P10, a stage during which CIs are undergoing apoptosis in *Lhx6* null mice (Figure 3A-D). Together, these observations suggest that deficits of MGE-derived CIs in *Lhx6* mutants are associated with enhanced network activity and brain excitability.

To explore the possibility that global changes in cellular microenvironment and brain activity can modulate the survival of CIs, we used the fluorescent reporter GFP to track CI precursors isolated from the basal forebrain of E14.5 GAD67::EGFP embryos (Tamamaki et al., 2003) following transplantation into the pallium of neonatal *Lhx6* mutant mice (Figure 3E). In this experimental paradigm the majority of

grafted CI precursors are eliminated by BAX-dependent apoptosis within 2 weeks, a feature that recapitulates the programmed cell death of endogenous CIs (Southwell et al., 2012). The number of transplanted GFP^+ CIs detected in the cortex of P16 *Lhx6*$^{-/-}$ animals two weeks after transplantation was significantly higher relative to that in *Lhx6*$^{+/-}$ controls (Figure 3F-K), suggesting that the documented increased network activity in the cortex of Lhx6-deficient mice enhances the survival and long-term integration of exogenous wild-type CIs into neuronal circuits of the host.

Cell autonomous increase in the activity of CIs enhances survival.

To directly test whether CI survival is regulated by neuronal activity in a cell autonomous manner, we transplanted CI precursors expressing Designer Receptors Exclusively Activated by Designer Drugs (DREADDs) and modulated their activity by administering appropriate ligands (Urban and Roth, 2015). Specifically, the MGE of E14.5 embryos was co-electroporated with a bi-cistronic expression vector encoding the hM3D(Gq) DREADD and Red Fluorescent Protein (RFP) and a control plasmid encoding GFP. Transfected CIs were mechanically dissociated and the resulting cell suspension grafted in the cortex of P0-P1 wild type mice. Since only a fraction of electroporated (GFP^+) neurons co-expressed hM3D(Gq) (RFP^+) (Figure 4A-E), the GFP^+RFP^- population served as an internal control for the effect of DREADD ligands. Indeed, administration of the DREADD ligand clozapine-N-oxide (CNO) selectively increased the activity of transfected GFP^+RFP^+ cells (Figure S6). Importantly, CNO treatment (administered twice daily from P14-P17) resulted in an increase in the fraction of GFP^+RFP^+ relative to GFP^+RFP^- cells when compared to vehicle administered littermates (Figure 4F-4J), suggesting that enhanced activity is sufficient to protect CIs from programmed cell death in an otherwise normal brain.

Together, our data provide evidence that neuronal activity modulates the number of CIs in the cortex in a cell autonomous manner.

Discussion

Distinct physiological mechanisms, collectively referred to as homeostatic plasticity, operate in the nervous system to maintain or restore the balance between excitation and inhibition, even after considerable disruption of network dynamics (Turrigiano, 2012). However, it is becoming increasingly clear that developmental programs may also contribute in controlling excitation/inhibition balance (Bartolini et al., 2013). Here, we provide evidence that neuronal activity during a critical developmental period of postnatal life gates the number of CIs in a homeostatic manner by modulating their programmed cell death. Our experiments highlight a critical interplay between the physiological state of the network and the number of its cellular constituents and suggest a feedback mechanism that fine-tunes the size of the CI population to stabilise brain activity.

Early stages of neural development are often characterised by large-scale proliferative expansion of progenitors and the generation of surplus number of neurons, which are eliminated at later stages by apoptosis in order to meet the physiological requirements of the system. For example, the size of motor neuron and sympathetic neuron pools is largely determined during development by the availability of limiting amounts of retrograde pro-survival signals supplied by appropriate peripheral targets (Oppenheim, 1991; Davies, 2003). The neurotrophic theory, despite being successful in the peripheral nervous system, cannot explain the regulation of apoptosis in most regions of the CNS where alternative pathways have been implicated (Dekkers et al., 2013). Earlier *in vivo* and *in vitro* studies have

demonstrated that survival of cortical PNs is enhanced by network activity and that NMDA receptor-mediated changes in synaptic activity modulate rates of apoptosis [Heck et al., 2008; Ikonomidou et al., 1999; Leveille et al., 2008; Verhage et al., 2000; reviewed in (Bell and Hardingham, 2011)]. In addition, apoptosis of adult-generated neurons, such as olfactory bulb interneurons and dentate gyrus granule cells, can be dramatically influenced by the activity of the mature networks they integrate into (Bovetti et al., 2009; Corotto et al., 1994; Mu et al., 2015; Petreanu and Alvarez-Buylla, 2002; Rochefort et al., 2002; Tashiro et al., 2006), probably through a cell autonomous mechanism (Lin et al., 2010). Contrasting these studies, Southwell and colleagues demonstrated recently that in rodents a large fraction of CIs (~40%) generated in the basal forebrain during development are eliminated during a critical early postnatal period by a program of apoptosis that is intrinsic to this cell lineage (Southwell et al., 2012). Using genetic lineage tracing in *Lhx6* mutants, we provide evidence that CI apoptosis in the postnatal brain is not predetermined but instead is modulated by the levels of network activity. This view is further supported by transplantation studies demonstrating that grafting of wild-type CI progenitors into the hyperactive cortex of Lhx6-deficient animals enhances their survival. Importantly, chemogenetic activation of CIs during a period of cortical circuit formation suggested that in the pallium inhibitory neurons monitor the activity in their microenvironment and adjust the level of apoptosis in a cell-autonomous manner. The intracellular cascades transducing network activity into CI survival remain unclear. However, the enhanced apoptosis of immature CIs observed in response to pharmacological inhibition of NMDA receptor (Roux et al., 2015) implicates excitatory glutamatergic neurotransmission in this regulatory pro-survival response. Our own transcriptomic

analysis identifies a set of candidate genes whose potential role in activity regulated apoptosis warrants further investigation.

To what extent changes in cortical network activity are implicated in the apparent compensatory response of CIs in other genetic backgrounds, remains unclear. Deletion of the Lhx6-dependent effector gene *Sox6* in postmitotic immature interneurons was associated with a dramatic decrease in the number of PV^+ and SST^+ interneurons, without an obvious change in the total number of CIs (Azim et al., 2009; Batista-Brito et al., 2009). Although an increase of NPY^+ interneurons was reported in these studies, the mechanisms that maintain the total number of CIs in Sox6 mutants remain unclear. Also, conditional inactivation of the orphan nuclear receptor COUP-TFI in interneuron progenitors resulted in decreased number of CR^+ and VIP^+ CIs and a concomitant increase of PV- and NPY-expressing subtypes, without affecting the total number of GABAergic interneurons in the cortex (Lodato et al., 2011). Although the authors proposed that this compensation is due to enhanced CI progenitor proliferation, it is possible that changes in apoptosis may also have contributed to this phenotype. We suggest that gene mutations that compromise the number or activity of specific CI subsets generally result in increased representation of counterpart subpopulations that are spared by the particular genetic modification and argue that this compensatory response is often mediated by sublineage-specific regulation of apoptosis.

Interestingly, it appears that only certain subtypes of CIs regulate their rate of apoptosis. For example, among the Lhx6-independent CGE-generated CIs only $Reelin^+$ neurons increase in number following *Lhx6* deletion. The subtype-specific response of CIs to network activity is not restricted to apoptosis as recent studies have shown that silencing CGE-derived interneurons results in defects in radial migration,

cell morphology and synaptic development of Reelin$^+$ but not VIP$^+$ CIs (De Marco Garcia et al., 2011; De Marco Garcia et al., 2015). The heterogeneous response of CI subtypes to ongoing network activity during development could have important implication for the establishment of the repertoire and connectivity pattern of local circuits in the cortex. Specifically, regional differences in activity patterns in the developing brain (Allene et al., 2008; Allene et al., 2012; Khazipov et al., 2004) may be responsible for the variability in the number and repertoire of CIs found in the mature cortex. Exploring the relationship between brain activity and CI repertoire will provide important insight into how local circuits are assembled.

In the last decade, several groups have established preclinical models of CI-based cell therapies to treat epileptic seizures (Alvarez Dolado and Broccoli, 2011; Southwell et al., 2014; Tyson and Anderson, 2014). Our present data argue that increased activity levels in the host brain, typically observed in epileptic encephalopathy mouse models (Batista-Brito et al., 2009; Hedrich et al., 2014), provide a favourable microenvironment for the survival of grafted immature CIs. By characterizing the pro-survival patterns of neuronal activity and identifying the CI subtypes best suited for transplantation would improve the effectiveness of these nascent therapies.

References

Allene, C., Cattani, A., Ackman, J.B., Bonifazi, P., Aniksztejn, L., Ben-Ari, Y., and Cossart, R. (2008). Sequential generation of two distinct synapse-driven network patterns in developing neocortex. J Neurosci 28, 12851-12863.

Allene, C., Picardo, M.A., Becq, H., Miyoshi, G., Fishell, G., and Cossart, R. (2012). Dynamic changes in interneuron morphophysiological properties mark the maturation of hippocampal network activity. J Neurosci 32, 6688-6698.

Alvarez Dolado, M., and Broccoli, V. (2011). GABAergic neuronal precursor grafting: implications in brain regeneration and plasticity. Neural Plast 2011, 384216.

Azim, E., Jabaudon, D., Fame, R.M., and Macklis, J.D. (2009). SOX6 controls dorsal progenitor identity and interneuron diversity during neocortical development. Nat Neurosci 12, 1238-1247.

Bartolini, G., Ciceri, G., and Marin O. (2013). Integration of GABAergic interneurons into cortical cell assemblies: Lessons from embryos and adults. Neuron 79, 849-864.

Batista-Brito, R., Rossignol, E., Hjerling-Leffler, J., Denaxa, M., Wegner, M., Lefebvre, V., Pachnis, V., and Fishell, G. (2009). The cell-intrinsic requirement of Sox6 for cortical interneuron development. Neuron 63, 466-481.

Bell, K.F., and Hardingham, G.E. (2011). The influence of synaptic activity on neuronal health. Curr Opin Neurobiol 21, 299-305.

Bovetti S., Veyrac, A., Peretto, P., Fasolo, A., and De Marchis S. (2009). Olfactory enrichment influences adult neurogenesis modulating GAD67 and plasticity-related molecules expression in newborn cells of the olfactory bulb. PlosOne 7, 1-10.

Corotto, F.S., Henegar, J.R., and Maruniak, J.A. (1994). Odor deprivation leads to reduced neurogenesis and reduced neuronal survival in the olfactory bulb of the adult mouse. Neuroscience 61, 739-744.

Davies, A.M. (2003). Regulation of neuronal survival and death by extracellular signals during development. EMBO J 22, 2537-2545.

De Marco Garcia, N.V., Karayannis, T., and Fishell, G. (2011). Neuronal activity is required for the development of specific cortical interneuron subtypes. Nature 472, 351-355.

De Marco Garcia, N.V., Priya, R., Tuncdemir, S.N., Fishell, G., and Karayannis, T. (2015). Sensory inputs control the integration of neurogliaform interneurons into cortical circuits. Nat Neurosci 18, 393-401.

Dekkers, M.P., Nikoletopoulou, V., and Barde, Y.A. (2013). Cell biology in neuroscience: Death of developing neurons: new insights and implications for connectivity. J Cell Biol 203, 385-393.

Fishell, G., and Rudy, B. (2011). Mechanisms of inhibition within the telencephalon: "where the wild things are". Annu Rev Neurosci 34, 535-567.

Gelman, D., Griveau, A., Dehorter, N., Teissier, A., Varela, C., Pla, R., Pierani, A., and Marin, O. (2011). A wide diversity of cortical GABAergic interneurons derives from the embryonic preoptic area. J Neurosci 31, 16570-16580.

Heck, N., Golbs, A., Riedemann, T., Sun, J.J., Lessmann, V., and Luhmann, H.J. (2008). Activity-dependent regulation of neuronal apoptosis in neonatal mouse cerebral cortex. Cereb Cortex 18, 1335-1349.

Hedrich, U.B., Liautard, C., Kirschenbaum, D., Pofahl, M., Lavigne, J., Liu, Y., Theiss, S., Slotta, J., Escayg, A., Dihne, M., *et al.* (2014). Impaired action potential initiation in GABAergic interneurons causes hyperexcitable networks in an epileptic mouse model carrying a human Na(V)1.1 mutation. J Neurosci 34, 14874-14889.

Ikonomidou, C., Bosch, F., Miksa, M., Bittigau, P., Vockler, J., Dikranian, K., Tenkova, T.I., Stefovska, V., Turski, L., and Olney, J.W. (1999). Blockade of NMDA receptors and apoptotic neurodegeneration in the developing brain. Science 283, 70-74.

Khazipov, R., Sirota, A., Leinekugel, X., Holmes, G.L., Ben-Ari, Y., and Buzsaki, G. (2004). Early motor activity drives spindle bursts in the developing somatosensory cortex. Nature 432, 758-761.

Kepecs, A., and Fishell, G. (2014). Interneuron cell types are fit to function. Nature 505, 318-326.

Kessaris, N., Fogarty, M., Iannarelli, P., Grist, M., Wegner, M., and Richardson, W.D. (2006). Competing waves of oligodendrocytes in the forebrain and postnatal elimination of an embryonic lineage. Nat Neurosci 9, 173-179.

Lee, S., Hjerling-Leffler, J., Zagha, E., Fishell, G., and Rudy, B. (2010). The largest group of superficial neocortical GABAergic interneurons expresses ionotropic serotonin receptors. J Neurosci 30, 16796-16808.

Leveille, F., El Gaamouch, F., Gouix, E., Lecocq, M., Lobner, D., Nicole, O., and Buisson, A. (2008). Neuronal viability is controlled by a functional relation between synaptic and extrasynaptic NMDA receptors. FASEB J 22, 4258-4271.

Lin, C.W., Sim, S., Ainsworth, A., Okada, M., Kelsch, W., and Lois, C. (2010). Genetically increased cell-intrinsic excitability enhances neuronal integration into adult brain circuits. Neuron 65, 32-39.

Liodis, P., Denaxa, M., Grigoriou, M., Akufo-Addo, C., Yanagawa, Y., and Pachnis, V. (2007). Lhx6 activity is required for the normal migration and specification of cortical interneuron subtypes. J Neurosci 27, 3078-3089.

Lodato, S., Tomassy, G.S., De Leonibus, E., Uzcategui, Y.G., Andolfi, G., Armentano, M., Touzot, A., Gaztelu, J.M., Arlotta, P., Menendez de la Prida, L., and Studer, M. (2011). Loss of COUP-TFI alters the balance between caudal ganglionic

eminence- and medial ganglionic eminence-derived cortical interneurons and results in resistance to epilepsy. J Neurosci 31, 4650-4662.

Madisen, L., Zwingman, T.A., Sunkin, S.M., Oh, S.W., Zariwala, H.A., Gu, H., Ng, L.L., Palmiter, R.D., Hawrylycz, M.J., Jones, A.R., *et al.* (2010). A robust and high-throughput Cre reporting and characterization system for the whole mouse brain. Nat Neurosci 13, 133-140.

Marin, O. (2012). Interneuron dysfunction in psychiatric disorders. Nat Rev Neurosci 13, 107-120.

Miller, M.W. (1995). Relationship of the time of origin and death of neurons in rat somatosensory cortex: barrel versus septal cortex and projection versus local circuit neurons. J Comp Neurol 355, 6-14.

Miyoshi, G., and Fishell, G. (2011). GABAergic interneuron lineages selectively sort into specific cortical layers during early postnatal development. Cereb Cortex 21, 845-852.

Mu, Y., Zhao, C., Toni, N., Yao, J., and Gage, F.H. (2015). Distinct roles of NMDA receptors at different stages of granule cell development in the adult brain. Elife 4, e07871.

Neves, G., Shah, M.M., Liodis, P., Achimastou, A., Denaxa, M., Roalfe, G., Sesay, A., Walker, M.C., and Pachnis, V. (2013). The LIM homeodomain protein Lhx6 regulates maturation of interneurons and network excitability in the mammalian cortex. Cereb Cortex 23, 1811-1823.

Oppenheim, R.W. (1991). Cell death during development of the nervous system. Annu. Rev. Neurosci. 14, 453–501

Petreanu, L., and Alvarez-Buylla, A. (2002). Maturation and Death of Adult-Born Olfactory Bulb Granule Neurons: Role of Olfaction. J Neurosci 22, 6106-6113.

Rochefort, C., Gheusi, G., Vincent, J.D., and Lledo, P.M. (2002). Enriched odor exposure increases the number of newborn neurons in the adult olfactory bulb and improves odor memory. J Neurosci 22, 2679-2689.

Roux, C., Aligny, C., Lesueur, C., Girault, V., Brunel, V., Ramdani, Y., Genty, D., Driouich, A., Laquerriere, A., Marret, S., *et al.* (2015). NMDA receptor blockade in the developing cortex induces autophagy-mediated death of immature cortical GABAergic interneurons: An ex vivo and in vivo study in Gad67-GFP mice. Exp Neurol 267, 177-193.

Rubenstein, J.L., and Merzenich, M.M. (2003). Model of autism: increased ratio of excitation/inhibition in key neural systems. Genes Brain Behav 2, 255-267.

Southwell, D.G., Nicholas, C.R., Basbaum, A.I., Stryker, M.P., Kriegstein, A.R., Rubenstein, J.L., and Alvarez-Buylla, A. (2014). Interneurons from embryonic development to cell-based therapy. Science 344, 1240622.

Southwell, D.G., Paredes, M.F., Galvao, R.P., Jones, D.L., Froemke, R.C., Sebe, J.Y., Alfaro-Cervello, C., Tang, Y., Garcia-Verdugo, J.M., Rubenstein, J.L., *et al.* (2012). Intrinsically determined cell death of developing cortical interneurons. Nature 491, 109-113.

Tamamaki, N., Yanagawa, Y., Tomioka, R., Miyazaki, J., Obata, K., and Kaneko, T. (2003). Green fluorescent protein expression and colocalization with calretinin, parvalbumin, and somatostatin in the GAD67-GFP knock-in mouse. J Comp Neurol 467, 60-79.

Tashiro, A., Sandler, V.M., Toni, N., Zhao, C., and Gage, F.H. (2006). NMDA-receptor-mediated, cell-specific integration of new neurons in adult dentate gyrus. Nature 442, 929-933.

Turrigiano, G. (2012). Homeostatic synaptic plasticity: local and global mechanisms for stabilizing neuronal function. Cold Spring Harb Perspect Biol 4, a005736.

Tyson, J.A., and Anderson, S.A. (2014). GABAergic interneuron transplants to study development and treat disease. Trends Neurosci 37, 169-177.

Urban, D.J., and Roth, B.L. (2015). DREADDs (designer receptors exclusively activated by designer drugs): chemogenetic tools with therapeutic utility. Annu Rev Pharmacol Toxicol 55, 399-417.

Verhage, M., Maia, A.S., Plomp, J.J., Brussaard, A.B., Heeroma, J.H., Vermeer, H., Toonen, R.F., Hammer, R.E., van den Berg, T.K., Missler, M., *et al.* (2000). Synaptic assembly of the brain in the absence of neurotransmitter secretion. Science 287, 864-869.

Vogt, D., Hunt, R.F., Mandal, S., Sandberg, M., Silberberg, S.N., Nagasawa, T., Yang, Z., Baraban, S.C., and Rubenstein, J.L. (2014). Lhx6 directly regulates Arx and CXCR7 to determine cortical interneuron fate and laminar position. Neuron 82, 350-364.

Vong, L., Ye, C., Yang, Z., Choi, B., Chua, S., Jr., and Lowell, B.B. (2011). Leptin action on GABAergic neurons prevents obesity and reduces inhibitory tone to POMC neurons. Neuron 71, 142-154.

Welagen, J., and Anderson, S.A. (2011). Origins of neocortical interneurons in mice. Dev Neurobiol 71, 10-17.

Wonders, C.P., and Anderson, S.A. (2006). The origin and specification of cortical interneurons. Nat Rev Neurosci 7, 687-696.

Yamaguchi, Y., and Miura, M. (2015). Programmed cell death in neurodevelopment. Dev Cell 32, 478-490.

Yu, H., Su, Y., Shin, J., Zhong, C., Guo, J.U., Weng, Y.L., Gao, F., Geschwind, D.H., Coppola, G., Ming, G.L., and Song, H. (2015). Tet3 regulates synaptic transmission and homeostatic plasticity via DNA oxidation and repair. Nat Neurosci 18, 836-843.

Zhao, Y., Flandin, P., Long, J.E., Cuesta, M.D., Westphal, H., and Rubenstein, J.L. (2008). Distinct molecular pathways for development of telencephalic interneuron subtypes revealed through analysis of Lhx6 mutants. J Comp Neurol 510, 79-99.

Figure Legends

Figure 1: Fate mapping reveals reduced viability of *Lhx6*-deficient MGE CIs and increased survival of CGE CIs, thus maintaining the total CI number found in P18 cortices constant. (**A-F**) tdT^+ (white signal) CIs in sections from the somatosensory cortex of *Lhx6* control (Ctrl, **A,C,E**) and mutant (Mut, **B,D,F**) P18 mice, fate-mapped using different Cre driver lines, as indicated in the panels. (**A,B**) MGE-derived, (**C,D**) all CIs, and (**E,F**) CGE-derived. (**G-I**) Quantification (normalised to the average control level) of tdT^+ cell density in somatosensory cortices of animals represented in A/B (**G**), C/D (**H**) and E/F (**I**). (**J-M**) Quantification of cell densities of CGE-derived $Reelin^+$ (**J**), CGE-derived VIP^+ (**K**), non-MGE-derived Pv^+ (**L**) and non-MGE-derived Sst^+ (**M**). Similar results were observed in the Motor Cortex (Suppl. Fig. 2). Data expressed as mean ± SEM. Statistical significance evaluated using Student's t-test, * denotes $p < 0.05$, ** $p<0.005$.

Figure 2: Reduced apoptosis of CGE CIs compensates for the loss of *Lhx6*-deficient MGE counterparts. CI subtypes in *Lhx6* control and mutant mice. (**A-H**) tdT-expressing CIs in cortical sections from P2 (**A-D**) and P7 (**E-H**) *Lhx6* control (**A,C,E,G**) and mutant (**B,D,F,H**) mice. tdT expression identifies CGE-derived (**A,B,E,F**) and MGE-derived CIs (**C,D,G,H**) respectively. (**I**) Quantification of CGE (close circles) and MGE (open circles) CI density in the whole cortex of *Lhx6* mutant mice relative to *Lhx6* controls (dotted line) at P2, P7 and P18. (**J**) Representative cortical section from P7 control mice showing MGE derived CIs (in red) and $TUNEL^+$ (green) cells. Yellow arrowheads indicate $TUNEL^+$ MGE derived CIs. (**K**,**L**) Quantification of MGE (**K**) and CGE (**L**) CIs undergoing apoptosis ($TUNEL^+$) in the cortex of *Lhx6* control and mutant P7 mice.

Figure 3: Hyperactivity of *Lhx6* mutants promotes CI progenitor survival. (**A,B**) Coronal sections from the hippocampal area of *Lhx6*$^{+/-}$ (**A**) and *Lhx6*$^{-/-}$ (**B**) P10 mice immunostained for c-fos. (**C, D**) *In situ* hybridization of somatosensory cortex sections from *Lhx6*$^{+/-}$ (**C**) and *Lhx6*$^{-/-}$ (**D**) P10 mice with an Arc riboprobe. **(E)** Schematic representation of the CI progenitor transplantation into the cortex of P0-P2 pups. (**F-I**) Coronal brain sections of Lhx6$^{+/-}$ (**F,G**) and Lhx6$^{-/-}$ (**H,I**) P16 mice transplanted at P0-P2 with wild-type GFP^{+} CI progenitors. Sections shown in **F**,**H** are more anterior to those shown in **G**,**I**. (**J**) Quantification of surviving GFP^{+} CIs in the cortex of one *Lhx6*$^{+/-}$ (black bars) and *Lhx6*$^{-/-}$ (red bars) littermate pair of P16 mice grafted with CI precursors at P0-P2. The rostro-caudal level of the forebrain that corresponds to each pair of black/red bars is shown schematically on the left. (**K)** Quantification of surviving GFP^{+} CIs in the cortex of *Lhx6*$^{+/-}$ and *Lhx6*$^{-/-}$ P16 mice. Values for the mutants (*Lhx6*$^{-/-}$) (circles) are normalized to the average value in control littermates (*Lhx6*$^{+/-}$; coloured bars represent SEM for individual grafting experiments). The number of GFP^{+} cells found in *Lhx6*$^{-/-}$ was 181 ± 13% higher in comparison to control littermates (p=0.02 one sample t-test (mean 100), n= 3 *Lhx6*$^{-/-}$, 10 *Lhx6*$^{+/-}$).

Figure 4: Cell autonomous depolarization of CIs enhances their survival. (**A**) Schematic representation of brain acute slice electroporation, grafting and vehicle/CNO administration protocol. Drug administration was targeted to coincide with the peak of apoptosis of transplanted CI progenitors. (**B)** Coronal section from an E14.5 embryo brain transfected with CAG:IRES:GFP (pGFP) and CAG:hM3D(Gq):IRES:RFP (pDREADRFP) plasmids and cultured for 12 h. Boxed area is magnified to show expression of both fluorescent reporters (**C**), GFP only (**D**)

and RFP only (**E**). (**F-I**) Representative sections from the somatosensory cortex of P17 mice grafted at P0-P2 with CI precursors transfected with pGFP and pDREADDRFP plasmids and injected with either vehicle (**F**) or CNO (**G**). Yellow arrowheads identify cells expressing both plasmids, while green arrows show cells expressing GFP only (**H,I**) Boxed region in **G** magnified to reveal expression of GFP (**H**) and RFP (**I**). (**J**) Quantification of RFP^+ cells found in the forebrain of P17 mice transplanted at P0-P2 (normalized to the total GFP^+ population). (RFP^+ - vehicle = 47 ± 3 %; CNO = 61 ± 3 %, p=0.01 Student's paired samples t-test, n= 3 vehicle, 3 CNO).

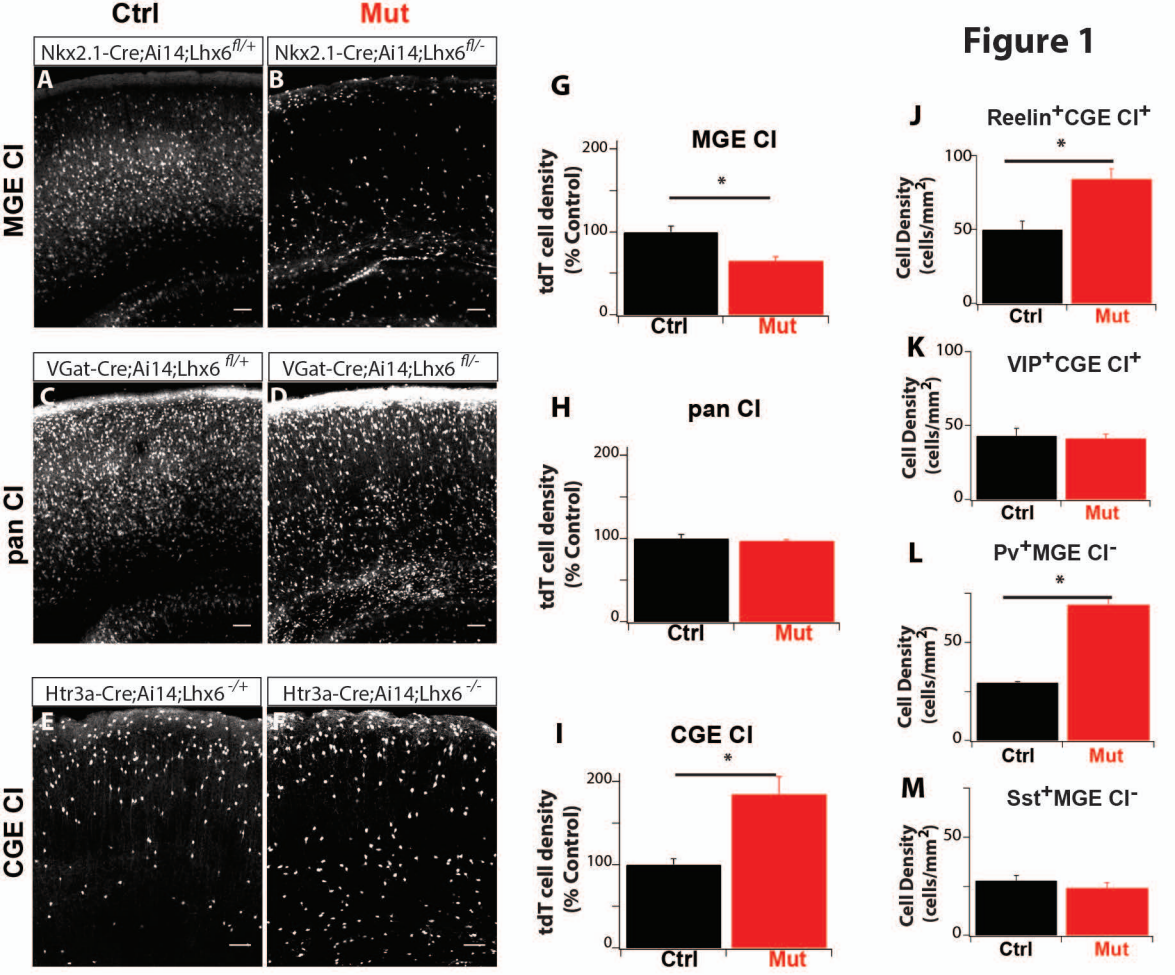
Figure 1
Ctrl
Mut
Nkx2.1-Cre;Ai14;Lhx6fl/+
Nkx2.1-Cre;Ai14;Lhx6fl/-
MGE CI
A
B
VGat-Cre;Ai14;Lhx6 fl/+
VGat-Cre;Ai14;Lhx6 fl/-
pan CI
C
D
Htr3a-Cre;Ai14;Lhx6 -/+
Htr3a-Cre;Ai14;Lhx6 -/-
CGE CI
E
F
G
MGE CI
tdT cell density (% Control)
200
100
0
*
Ctrl
Mut
H
pan CI
tdT cell density (% Control)
200
100
0
Ctrl
Mut
I
CGE CI
tdT cell density (% Control)
200
100
0
*
Ctrl
Mut
J
Reelin+CGE CI+
Cell Density (cells/mm2)
100
50
0
*
Ctrl
Mut
K
VIP+CGE CI+
Cell Density (cells/mm2)
100
50
0
Ctrl
Mut
L
Pv+MGE CI-
Cell Density (cells/mm2)
50
0
*
Ctrl
Mut
M
Sst+MGE CI-
Cell Density (cells/mm2)
50
0
Ctrl
Mut

Figure 2

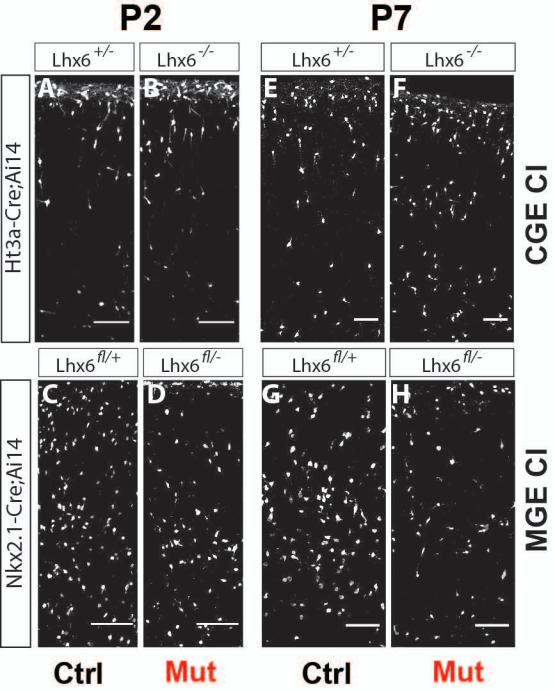
P2
P7
Lhx6 +/-
Lhx6 -/-
Lhx6 +/-
Lhx6 -/-
A
B
E
F
Ht3a-Cre;Ai14
CGE CI
Lhx6 fl/+
Lhx6 fl/-
Lhx6 fl/+
Lhx6 fl/-
C
D
G
H
Nkx2.1-Cre;Ai14
MGE CI
Ctrl
Mut
Ctrl
Mut

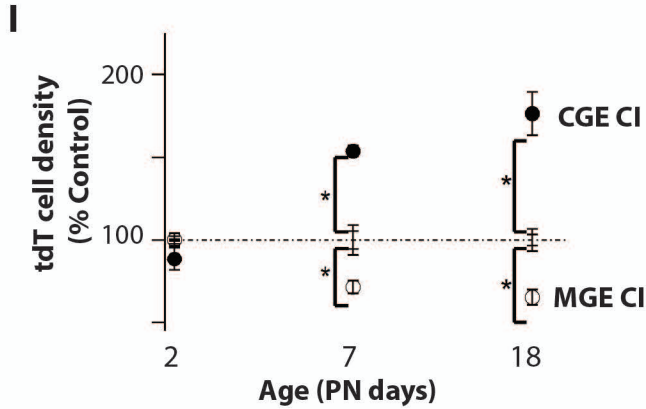
I
tdT cell density
(% Control)
200
100
CGE CI
MGE CI
*
*
*
*
2
7
18
Age (PN days)

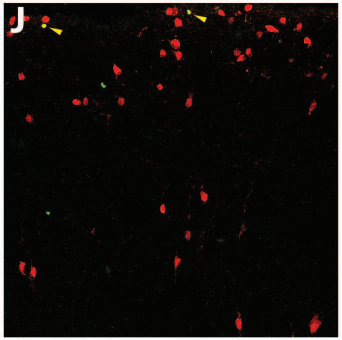
J

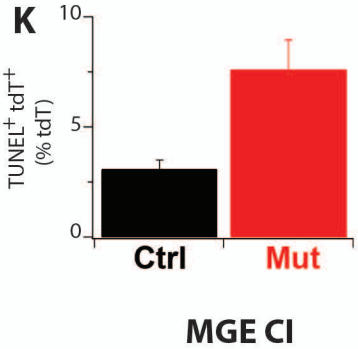
K
TUNEL+ tdT+
(% tdT)
10
5
0
Ctrl
Mut
MGE CI

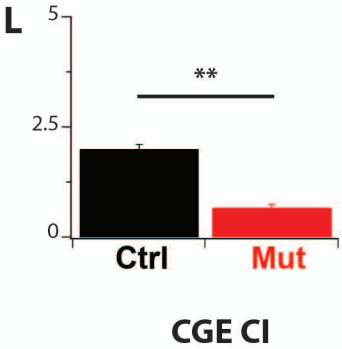
L
5
2.5
0
**
Ctrl
Mut
CGE CI

Figure 3

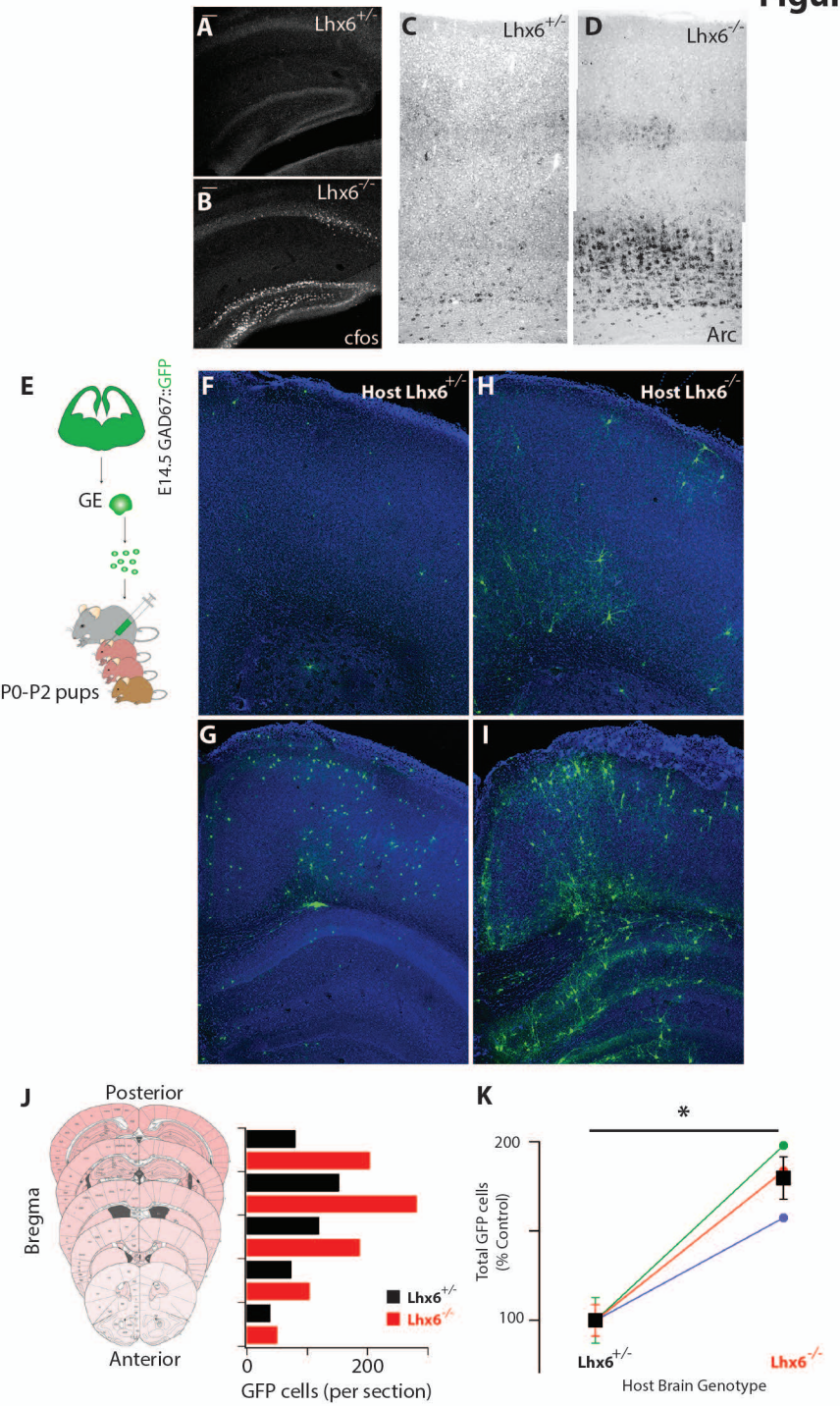
A
Lhx6+/-
B
Lhx6-/-
cfos
C
Lhx6+/-
D
Lhx6-/-
Arc
E
E14.5 GAD67::GFP
GE
P0-P2 pups
F
Host Lhx6+/-
H
Host Lhx6-/-
G
I
J
Posterior
Bregma
Anterior
Lhx6+/-
Lhx6-/-
0
200
GFP cells (per section)
K
*
200
100
Total GFP cells
(% Control)
Lhx6+/-
Lhx6-/-
Host Brain Genotype

Figure 4

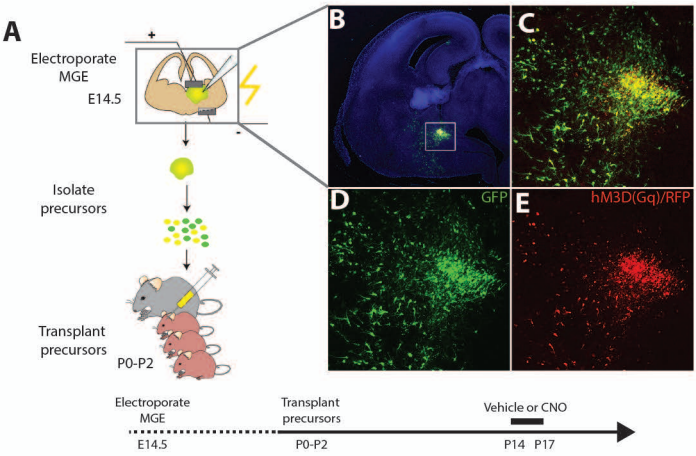
A
Electroporate MGE
E14.5
+
-
Isolate precursors
Transplant precursors
P0-P2
B
C
D
GFP
E
hM3D(Gq)/RFP
Electroporate MGE
E14.5
Transplant precursors
P0-P2
Vehicle or CNO
P14 P17

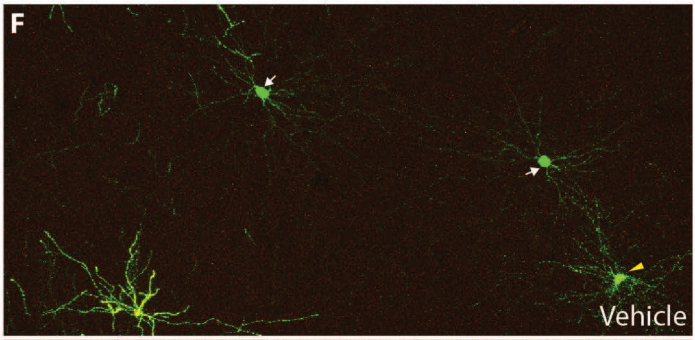
F
Vehicle

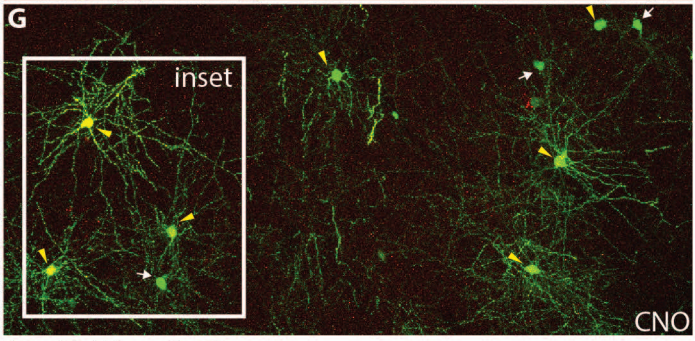
G
inset
CNO

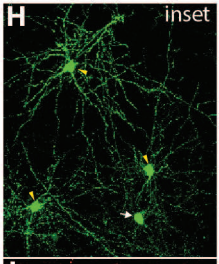
H
inset

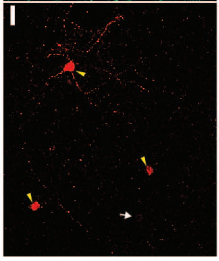
I

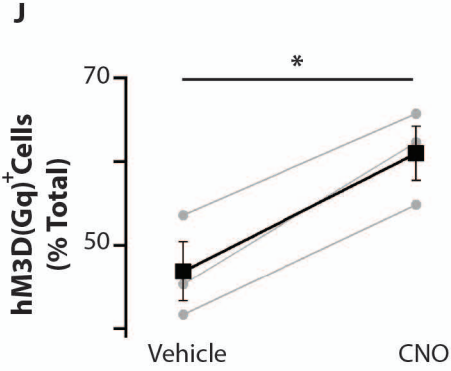
J
*
70
50
hM3D(Gq)+Cells
(% Total)
Vehicle
CNO